4

Adaptive Kalman Filter for Navigation Sensor Fusion

Dah-Jing Jwo, Fong-Chi Chung
National Taiwan Ocean University, Keelung
Taiwan

Tsu-Pin Weng
EverMore Technology, Inc., Hsinchu
Taiwan

1. Introduction

As a form of optimal estimator characterized by recursive evaluation, the Kalman filter (KF) (Bar-Shalom, et al, 2001; Brown and Hwang, 1997, Gelb, 1974; Grewal & Andrews, 2001) has been shown to be the filter that minimizes the variance of the estimation mean square error (MSE) and has been widely applied to the navigation sensor fusion. Nevertheless, in Kalman filter designs, the divergence due to modeling errors is critical. Utilization of the KF requires that all the plant dynamics and noise processes are completely known, and the noise process is zero mean white noise. If the input data does not reflect the real model, the KF estimates may not be reliable. The case that theoretical behavior of a filter and its actual behavior do not agree may lead to divergence problems. For example, if the Kalman filter is provided with information that the process behaves a certain way, whereas, in fact, it behaves a different way, the filter will continually intend to fit an incorrect process signal. Furthermore, when the measurement situation does not provide sufficient information to estimate all the state variables of the system, in other words, the estimation error covariance matrix becomes unrealistically small and the filter disregards the measurement.

In various circumstances where there are uncertainties in the system model and noise description, and the assumptions on the statistics of disturbances are violated since in a number of practical situations, the availability of a precisely known model is unrealistic due to the fact that in the modelling step, some phenomena are disregarded and a way to take them into account is to consider a nominal model affected by uncertainty. The fact that KF highly depends on predefined system and measurement models forms a major drawback. If the theoretical behavior of the filter and its actual behavior do not agree, divergence problems tend to occur. The adaptive algorithm has been one of the approaches to prevent divergence problem of the Kalman filter when precise knowledge on the models are not available.

To fulfil the requirement of achieving the filter optimality or to preventing divergence problem of Kalman filter, the so-called adaptive Kalman filter (AKF) approach (Ding, et al,

2007; El-Mowafy & Mohamed, 2005; Mehra, 1970, 1971, 1972; Mohamed & Schwarz, 1999; Hide et al., 2003) has been one of the promising strategies for dynamically adjusting the parameters of the supposedly optimum filter based on the estimates of the unknown parameters for on-line estimation of motion as well as the signal and noise statistics available data. Two popular types of the adaptive Kalman filter algorithms include the innovation-based adaptive estimation (IAE) approach (El-Mowafy & Mohamed, 2005; Mehra, 1970, 1971, 1972; Mohamed & Schwarz, 1999; Hide et al., 2003) and the adaptive fading Kalman filter (AFKF) approach (Xia et al., 1994; Yang, et al, 1999, 2004;Yang & Xu, 2003; Zhou & Frank, 1996), which is a type of covariance scaling method, for which suboptimal fading factors are incorporated. The AFKF incorporates suboptimal fading factors as a multiplier to enhance the influence of innovation information for improving the tracking capability in high dynamic maneuvering.

The Global Positioning System (GPS) and inertial navigation systems (INS) (Farrell, 1998; Salychev, 1998) have complementary operational characteristics and the synergy of both systems has been widely explored. GPS is capable of providing accurate position information. Unfortunately, the data is prone to jamming or being lost due to the limitations of electromagnetic waves, which form the fundamental of their operation. The system is not able to work properly in the areas due to signal blockage and attenuation that may deteriorate the overall positioning accuracy. The INS is a self-contained system that integrates three acceleration components and three angular velocity components with respect to time and transforms them into the navigation frame to deliver position, velocity and attitude components. For short time intervals, the integration with respect to time of the linear acceleration and angular velocity monitored by the INS results in an accurate velocity, position and attitude. However, the error in position coordinates increase unboundedly as a function of time. The GPS/INS integration is the adequate solution to provide a navigation system that has superior performance in comparison with either a GPS or an INS stand-alone system. The GPS/INS integration is typically carried out through the Kalman filter. Therefore, the design of GPS/INS integrated navigation system heavily depends on the design of sensor fusion method. Navigation sensor fusion using the AKF will be discussed. A hybrid approach will be presented and performance will be evaluated on the loosely-coupled GPS/INS navigation applications.

This chapter is organized as follows. In Section 2, preliminary background on adaptive Kalman filters is reviewed. An IAE/AFKF hybrid adaptation approach is introduced in Section 3. In Section 4, illustrative examples on navigation sensor fusion are given. Conclusions are given in Section 5.

2. Adaptive Kalman Filters

The process model and measurement model are represented as

$$\mathbf{x}_{k+1} = \mathbf{\Phi}_k \mathbf{x}_k + \mathbf{w}_k \tag{1a}$$

$$\mathbf{z}_k = \mathbf{H}_k \mathbf{x}_k + \mathbf{v}_k \tag{1b}$$

where the state vector $\mathbf{x}_k \in \Re^n$, process noise vector $\mathbf{w}_k \in \Re^n$, measurement vector $\mathbf{z}_k \in \Re^m$, and measurement noise vector $\mathbf{v}_k \in \Re^m$. In Equation (1), both the vectors $\mathbf{w}_k$ and $\mathbf{v}_k$ are zero mean Gaussian white sequences having zero crosscorrelation with each other:

$$\mathbf{E}[\mathbf{w}_k\mathbf{w}_i^{\mathrm{T}}]=\begin{cases}\mathbf{Q}_k, & i=k\\ 0, & i\neq k\end{cases};\ \mathbf{E}[\mathbf{v}_k\mathbf{v}_i^{\mathrm{T}}]=\begin{cases}\mathbf{R}_k, & i=k\\ 0, & i\neq k\end{cases};\ \mathbf{E}[\mathbf{w}_k\mathbf{v}_i^{\mathrm{T}}]=\mathbf{0} \qquad \textit{for all } i \textit{ and } k \quad (2)$$

where $\mathbf{Q}_k$ is the process noise covariance matrix, $\mathbf{R}_k$ is the measurement noise covariance matrix, $\mathbf{\Phi}_k = e^{\mathbf{F}\Delta t}$ is the state transition matrix, and Δt is the sampling interval, $E[\cdot]$ represents expectation, and superscript "T" denotes matrix transpose.

The discrete-time Kalman filter algorithm is summarized as follow:

Prediction steps/time update equations:

$$\hat{\mathbf{x}}_{k+1}^{-}=\mathbf{\Phi}_k\hat{\mathbf{x}}_k \quad (3)$$

$$\mathbf{P}_{k+1}^{-}=\mathbf{\Phi}_k\mathbf{P}_k\mathbf{\Phi}_k^{\mathrm{T}}+\mathbf{Q}_k \quad (4)$$

Correction steps/measurement update equations:

$$\mathbf{K}_k=\mathbf{P}_k^{-}\mathbf{H}_k^{\mathrm{T}}[\mathbf{H}_k\mathbf{P}_k^{-}\mathbf{H}_k^{\mathrm{T}}+\mathbf{R}_k]^{-1} \quad (5)$$

$$\hat{\mathbf{x}}_k=\hat{\mathbf{x}}_k^{-}+\mathbf{K}_k[\mathbf{z}_k-\mathbf{H}_k\hat{\mathbf{x}}_k^{-}] \quad (6)$$

$$\mathbf{P}_k=[\mathbf{I}-\mathbf{K}_k\mathbf{H}_k]\mathbf{P}_k^{-} \quad (7)$$

A limitation in applying Kalman filter to real-world problems is that the *a priori* statistics of the stochastic errors in both dynamic process and measurement models are assumed to be available, which is difficult in practical application due to the fact that the noise statistics may change with time. As a result, the set of unknown time-varying statistical parameters of noise, $\{\mathbf{Q}_k, \mathbf{R}_k\}$, needs to be simultaneously estimated with the system state and the error covariance. Two popular types of the adaptive Kalman filter algorithms include the innovation-based adaptive estimation (IAE) approach (El-Mowafy and Mohamed, 2005; Mehra, 1970, 1971, 1972; Mohamed and Schwarz, 1999; Hide et al., 2003; Caliskan & Hajiyev, 2000) and the adaptive fading Kalman filter (AFKF) approach (Xia et al., 1994; Zhou & Frank, 1996), which is a type of covariance scaling method, for which suboptimal fading factors are incorporated.

2.1 The innovation-based adaptive estimation

The innovation sequences have been utilized by the correlation and covariance-matching techniques to estimate the noise covariances. The basic idea behind the covariance-matching approach is to make the actual value of the covariance of the residual consistent with its theoretical value. The implementation of IAE based AKF to navigation designs has been widely explored (Hide *et al*, 2003, Mohamed and Schwarz 1999). Equations (3)-(4) are the time update equations of the algorithm from k to step $k+1$, and Equations (5)-(7) are the measurement update equations. These equations incorporate a measurement value into *a priori* estimation to obtain an improved *a posteriori* estimation. In the above equations, $\mathbf{P}_k$ is the error covariance matrix defined by $E[(\mathbf{x}_k-\hat{\mathbf{x}}_k)(\mathbf{x}_k-\hat{\mathbf{x}}_k)^{\mathrm{T}}]$, in which $\hat{\mathbf{x}}_k$ is an estimation of the system state vector $\mathbf{x}_k$, and the weighting matrix $\mathbf{K}_k$ is generally referred to as the Kalman gain matrix. The Kalman filter algorithm starts with an initial condition value, $\hat{\mathbf{x}}_0^{-}$ and $\mathbf{P}_0^{-}$. When new measurement $\mathbf{z}_k$ becomes available with the progression of time, the estimation of states and the corresponding error covariance would follow recursively ad infinity. Mehra (1970, 1971, 1972) classified the adaptive approaches into four categories: Bayesian, maximum likelihood, correlation and covariance matching. The innovation

sequences have been utilized by the correlation and covariance-matching techniques to estimate the noise covariances. The basic idea behind the covariance-matching approach is to make the actual value of the covariance of the residual consistent with its theoretical value.

From the incoming measurement $\mathbf{z}_k$ and the optimal prediction $\hat{\mathbf{x}}_k^-$ obtained in the previous step, the innovations sequence is defined as

$$\boldsymbol{\upsilon}_k = \mathbf{z}_k - \hat{\mathbf{z}}_k^- \tag{8}$$

The innovation reflects the discrepancy between the predicted measurement $\mathbf{H}_k\hat{\mathbf{x}}_k^-$ and the actual measurement $\mathbf{z}_k$. It represents the additional information available to the filter as a consequence of the new observation $\mathbf{z}_k$. The weighted innovation, $\mathbf{K}_k(\mathbf{z}_k - \mathbf{H}_k\hat{\mathbf{x}}_k^-)$, acts as a correction to the predicted estimate $\hat{\mathbf{x}}_k^-$ to form the estimation $\hat{\mathbf{x}}_k$. Substituting the measurement model Equation (1b) into Equation (8) gives

$$\boldsymbol{\upsilon}_k = \mathbf{H}_k(\mathbf{x}_k - \hat{\mathbf{x}}_k^-) + \mathbf{v}_k \tag{9}$$

which is a zero-mean Gaussian white noise sequence. An innovation of zero means that the two are in complete agreement. The mean of the corresponding error of an unbiased estimator is zero. By taking variances on both sides, we have the theoretical covariance, the covariance matrix of the innovation sequence is given by

$$\mathbf{C}_{\upsilon_k} = E[\boldsymbol{\upsilon}_k\boldsymbol{\upsilon}_k^{\mathrm{T}}] = \mathbf{H}_k\mathbf{P}_k^-\mathbf{H}_k^{\mathrm{T}} + \mathbf{R}_k \tag{10a}$$

which can be written as

$$\mathbf{C}_{\upsilon_k} = \mathbf{H}_k(\boldsymbol{\Phi}_k\mathbf{P}_k\boldsymbol{\Phi}_k^T + \boldsymbol{\Gamma}_k\mathbf{Q}_k\boldsymbol{\Gamma}_k^T)\mathbf{H}_k^{\mathrm{T}} + \mathbf{R}_k \tag{10b}$$

Defining $\hat{\mathbf{C}}_{\upsilon_k}$ as the statistical sample variance estimate of $\mathbf{C}_{\upsilon_k}$, matrix $\hat{\mathbf{C}}_{\upsilon_k}$ can be computed through averaging inside a moving estimation window of size N

$$\hat{\mathbf{C}}_{\upsilon_k} = \frac{1}{N}\sum_{j=j_0}^{k}\boldsymbol{\upsilon}_j\boldsymbol{\upsilon}_j^{\mathrm{T}} \tag{11}$$

where N is the number of samples (usually referred to the window size); $j_0 = k - N + 1$ is the first sample inside the estimation window. The window size N is chosen empirically (a good size for the moving window may vary from 10 to 30) to give some statistical smoothing. More detailed discussion can be referred to Gelb (1974), Brown & Hwang (1997), and Grewal & Andrews (2001).

The benefit of the adaptive algorithm is that it keeps the covariance consistent with the real performance. The innovation sequences have been utilized by the correlation and covariance-matching techniques to estimate the noise covariances. The basic idea behind the covariance-matching approach is to make the actual value of the covariance of the residual consistent with its theoretical value. This leads to an estimate of $\mathbf{R}_k$:

$$\hat{\mathbf{R}}_k = \hat{\mathbf{C}}_{\upsilon_k} - \mathbf{H}_k\mathbf{P}_k^-\mathbf{H}_k^{\mathrm{T}} \tag{12}$$

Based on the residual based estimate, the estimate of process noise $\mathbf{Q}_k$ is obtained:

$$\hat{\mathbf{Q}}_k = \frac{1}{N}\sum_{j=j_0}^{k}\Delta\mathbf{x}_j\Delta\mathbf{x}_j^{\mathrm{T}} + \mathbf{P}_k - \boldsymbol{\Phi}_k\mathbf{P}_{k-1}\boldsymbol{\Phi}_k^{\mathrm{T}} \tag{13}$$

where $\Delta \mathbf{x}_k = \mathbf{x}_k - \hat{\mathbf{x}}_k^-$. This equation can also be written in terms of the innovation sequence:

$$\hat{\mathbf{Q}}_k \approx \mathbf{K}_k \hat{\mathbf{C}}_{\upsilon_k} \mathbf{K}_k^{\mathrm{T}} \tag{14}$$

For more detailed information derivation for these equations, see Mohamed & Schwarz (1999).

2.2 The adaptive fading Kalman filter

The idea of fading memory is to apply a factor to the predicted covariance matrix to deliberately increase the variance of the predicted state vector. The main difference between different fading memory algorithms is on the calculation of the scale factor.

A. Typical adaptive fading Kalman filter

One of the approaches for adaptive processing is on the incorporation of fading factors. Xia et al. (1994) proposed a concept of adaptive fading Kalman filter (AFKF) and solved the state estimation problem. In the AFKF, suboptimal fading factors are introduced into the nonlinear smoother algorithm. The idea of fading Kalman filtering is to apply a factor matrix to the predicted covariance matrix to deliberately increase the variance of the predicted state vector. In the so called AFKF algorithm, suboptimal fading factors are introduced into the algorithm.

The idea of fading Kalman filtering is to apply a factor matrix to the predicted covariance matrix to deliberately increase the variance of the predicted state vector:

$$\mathbf{P}_{k+1}^- = \boldsymbol{\lambda}_k \boldsymbol{\Phi}_k \mathbf{P}_k \boldsymbol{\Phi}_k^T + \mathbf{Q}_k \tag{15a}$$

or

$$\mathbf{P}_{k+1}^- = \boldsymbol{\lambda}_k (\boldsymbol{\Phi}_k \mathbf{P}_k \boldsymbol{\Phi}_k^T + \mathbf{Q}_k) \tag{15b}$$

where $\boldsymbol{\lambda}_k = diag(\lambda_1, \lambda_2 \ldots, \lambda_m)$. The main difference between various fading memory algorithms is on the calculation of scale factor $\boldsymbol{\lambda}_k$. One approach is to assign the scale factors as constants. When $\lambda_i \le 1$ ($i = 1,2,\ldots,m$), the filtering is in a steady state processing while $\lambda_i > 1$, the filtering may tend to be unstable. For the case $\lambda_i = 1$, it deteriorates to the standard Kalman filter. There are some drawbacks with constant factors, e.g., as the filtering proceeds, the precision of the filtering will decrease because the effects of old data tend to become less and less. The ideal way is to use time-varying factors that are determined according to the dynamic and observation model accuracy.

To increase the tracking capability, the time-varying suboptimal scaling factor is incorporated, for on-line tuning the covariance of the predicted state, which adjusts the filter gain, and accordingly the improved version of AFKF is developed. The optimum fading factor is:

$$\lambda_k = \max\left\{1, \frac{tr[\mathbf{N}_k]}{tr[\mathbf{M}_k]}\right\} \tag{16}$$

Some other choices of the factors are also used:

$$\lambda_k = \max\left\{1, \frac{1}{n} tr[\mathbf{N}_k \mathbf{M}_k^{-1}]\right\};\ \lambda_k = \max\left\{1, \frac{\alpha}{n} tr[\mathbf{N}_k \mathbf{M}_k^{-1}]\right\};\ \lambda_k = \max\left\{1, \alpha \frac{tr[\mathbf{N}_k]}{tr[\mathbf{M}_k]}\right\}$$

where $tr[\cdot]$ is the trace of matrix. The parameters are given by

$$\mathbf{M}_k = \mathbf{H}_k \boldsymbol{\Phi}_k \mathbf{P}_k \boldsymbol{\Phi}_k^T \mathbf{H}_k^T \tag{17}$$

$$\mathbf{N}_k = \mathbf{C}_0 - \mathbf{R}_k - \mathbf{H}_k \mathbf{Q}_k \mathbf{H}_k^T \tag{18a}$$

where

$$\mathbf{C}_0 = \begin{cases} \dfrac{\boldsymbol{\upsilon}_0 \boldsymbol{\upsilon}_0^T}{2}, k = 0 \\ \dfrac{[\lambda_k \boldsymbol{\upsilon}_k \boldsymbol{\upsilon}_k^T]}{1+\lambda_k}, k \geq 1 \end{cases} \tag{19}$$

Equation (18a) can be modified by multiplying an innovation enhancement weighting factor γ, and adding an additional term:

$$\mathbf{N}_k = \gamma \mathbf{C}_0 - \mathbf{R}_k - \mathbf{H}_k \mathbf{Q}_k \mathbf{H}_k^T \tag{18b}$$

In the AFKF, the key parameter is the fading factor matrix $\boldsymbol{\lambda}_k$. The factor γ is introduced for increasing the tracking capability through the increased weighting of covariance matrix of the innovation. The value of weighting factor γ is tuned to improve the smoothness of state estimation. A larger weighting factor γ provides stronger tracking capability, which is usually selected empirically. The fading memory approach tries to estimate a scale factor to increase the predicted variance components of the state vector. The variance estimation method directly calculates the variance factor for the dynamic model.

There are some drawbacks with a constant factor, e.g., as the filtering proceeds, the precision of the filtering will decrease because the effects of old data will become less and less. The ideal way is to use a variant scale factor that will be determined based on the dynamic and observation model accuracy.

B. The strong tracking Kalman filter

Zhou & Frank (1996) proposed a concept of strong tracking Kalman filter (STKF) (Zhou & Frank, 1996; Jwo & Wang, 2007) and solved the state estimation problem of a class of nonlinear systems with white noise. In the so called STKF algorithm, suboptimal fading factors are introduced into the nonlinear smoother algorithm. The STKF has several important merits, including (1) strong robustness against model uncertainties; (2) good real-time state tracking capability even when a state jump occurs, no matter whether the system has reached steady state or not. Zhou et al proved that a filter is called the STKF only if the filter satisfies the orthogonal principle stated as follows:

Orthogonal principle: The sufficient condition for a filter to be called the STKF only if the time-varying filter gain matrix be selected on-line such that the state estimation mean-square error is minimized and the innovations remain orthogonal (Zhou & Frank, 1996):

$$E[\mathbf{x}_k - \hat{\mathbf{x}}_k][\mathbf{x}_k - \hat{\mathbf{x}}_k]^T = \min$$

$$E[\boldsymbol{\upsilon}_{k+j} \boldsymbol{\upsilon}_k^T] = 0, \; k = 0,1,2..., \; j = 1,2... \tag{20}$$

Equation (20) is required for ensuring that the innovation sequence will be remained orthogonal.

The time-varying suboptimal scaling factor is incorporated, for on-line tuning the covariance of the predicted state, which adjusts the filter gain, and accordingly the STKF is developed. The suboptimal scaling factor in the time-varying filter gain matrix is given by:

$$\lambda_{i,k} = \begin{cases} \alpha_i c_k & ,\alpha_i c_k \geq 1 \\ 1 & ,\alpha_i c_k < 1 \end{cases} \tag{21}$$

where

$$c_k = \frac{tr[\mathbf{N}_k]}{tr[\boldsymbol{\alpha}\mathbf{M}_k]} \tag{22}$$

and

$$\mathbf{N}_k = \boldsymbol{\gamma}\mathbf{V}_k - \beta\mathbf{R}_k - \mathbf{H}_k\mathbf{Q}_k\mathbf{H}_k^T \tag{23}$$

$$\mathbf{M}_k = \mathbf{H}_k\boldsymbol{\Phi}_k\mathbf{P}_k\boldsymbol{\Phi}_k^T\mathbf{H}_k^T \tag{24}$$

$$\mathbf{V}_k = \begin{cases} \boldsymbol{\upsilon}_0\boldsymbol{\upsilon}_0^T, k = 0 \\ \dfrac{[\rho\mathbf{V}_{k-1} + \boldsymbol{\upsilon}_k\boldsymbol{\upsilon}_k^T]}{1+\rho}, k \geq 1 \end{cases} \tag{25}$$

The key parameter in the STKF is the fading factor matrix $\boldsymbol{\lambda}_k$, which is dependent on three parameters, including (1) α_i; (2) the forgetting factor (ρ); (3) and the softening factor (β). These parameters are usually selected empirically. $\alpha_i \geq 1, i = 1,2,\ldots,m$, which are *a priori* selected. If from *a priori* knowledge, we have the knowledge that $\mathbf{x}$ will have a large change, then a large α_i should be used so as to improve the tracking capability of the STKF. On the other hand, if no *a priori* knowledge about the plant dynamic, it is commonly select $\alpha_1 = \alpha_2 = \cdots = \alpha_m = 1$. In such case, the STKF based on multiple fading factors deteriorates to a STKF based on a single fading factor. The range of the forgetting factor is $0 < \rho \leq 1$, for which 0.95 is commonly used. The softening factor β is utilized to improve the smoothness of state estimation. A larger β (with value no less than 1) leads to better estimation accuracy; while a smaller β provides stronger tracking capability. The value is usually determined empirically through computer simulation and $\beta = 4.5$ is a commonly selected value.

C. The algorithm proposed by Yang, et al.

An adaptive factor depending on the discrepancy between predicted state from the dynamic model and the geometric estimated state by using measurements was proposed by Yang et al (1999, 2003, 2004), where they introduced an adaptive factor α incorporated into for regulating the error covariance

$$\mathbf{P}_{k+1}^{-} = (\boldsymbol{\Phi}_k\mathbf{P}_k\boldsymbol{\Phi}_k^{\mathrm{T}} + \mathbf{Q}_k)/\alpha \tag{26}$$

where α is the single factor given by

$$\alpha = \begin{cases} 1 & |\tilde{\boldsymbol{\upsilon}}_k| \leq c_0 \\ \dfrac{c_0}{|\tilde{\boldsymbol{\upsilon}}_k|}\left(\dfrac{c_1 - |\tilde{\boldsymbol{\upsilon}}_k|}{c_1 - c_0}\right)^2 & c_0 < |\tilde{\boldsymbol{\upsilon}}_k| \leq c_1 \\ 0 & |\tilde{\boldsymbol{\upsilon}}_k| > c_1 \end{cases} \tag{27}$$

It is seen that Equation (15a) with $\lambda_k = 1/\alpha$ results in Equation (26). In Equation (27), $c_0 = 1$ and $c_1 = 3$ are commonly selected values, and

$$\tilde{\upsilon}_k = \frac{\|\upsilon_k\|}{\sqrt{\mathbf{C}_{\upsilon_k}}} \tag{28}$$

To avoid $\alpha = 0$, it is common to choose

$$\alpha = \begin{cases} 1 & |\tilde{\upsilon}_k| \le c \\ \dfrac{c}{|\tilde{\upsilon}_k|} & |\tilde{\upsilon}_k| > c \end{cases} \tag{29}$$

The *a priori* selected value α is usually selected empirically. If from *a priori* knowledge, we have the knowledge that $\mathbf{x}$ will have a large change, then a small α should be used so as to improve the tracking capability. The range of the factor is $0 < \alpha \le 1$. The factor is utilized to improve the smoothness of state estimation. A larger α (≤ 1) leads to better estimation accuracy; while a smaller α provides stronger tracking capability. The value is usually determined empirically through personal experience or computer simulation using a heuristic searching scheme. In the case that $\alpha = 1$, it deteriorates to a standard Kalman filter. In Equation (29), the threshold $c = 0.5$ is an average value commonly used. To increase the tracking capability, the time-varying suboptimal scaling factor need to be properly designed, for on-line tuning the covariance of the predicted state, which adjusts the filter gain, and accordingly the improved version of AFKF is able to provide better estimation accuracy.

2.3 The tuning logic for parameter adaptation

Another type of adaptation can be conducted by introducing a scaling factor directly to the $\mathbf{Q}_k$ and/or $\mathbf{R}_k$ matrices. To account for the greater uncertainty, the covariances need to be updated, through one of the following ways (Bakhache & Nikiforov, 2000; Jwo & Cho, 2007; Sasiadek, et al, 2000):

(1) $\mathbf{Q}_k \to \mathbf{Q}_{k-1} + \Delta\mathbf{Q}_k$; $\mathbf{R}_k \to \mathbf{R}_{k-1} + \Delta\mathbf{R}_k$

(2) $\mathbf{Q}_k \to \mathbf{Q}_k \alpha^{-(k+1)}$; $\mathbf{R}_k \to \mathbf{R}_k \beta^{-(k+1)}$, $\alpha \ge 1$; $\beta \ge 1$

(3) $\mathbf{Q}_k \to \alpha\mathbf{Q}_k$; $\mathbf{R}_k \to \beta\mathbf{R}_k$

For example, if (3) is utilized as an example, the filter equations can be augmented in the following way:

$$\mathbf{P}_{k+1}^{-} = \mathbf{\Phi}_k \mathbf{P}_k \mathbf{\Phi}_k^{\mathrm{T}} + \alpha\mathbf{Q}_k \tag{30}$$

$$\mathbf{K}_k = \mathbf{P}_k^{-}\mathbf{H}_k^{\mathrm{T}}[\mathbf{H}_k\mathbf{P}_k^{-}\mathbf{H}_k^{\mathrm{T}} + \beta\mathbf{R}_k]^{-1}$$

In case that $\alpha = \beta = 1$, it deteriorates to the standard Kalman filter.

To detect the discrepancy between $\hat{\mathbf{C}}_{\upsilon_k}$ and $\mathbf{C}_{\upsilon_k}$, we define the degree of mismatch (DOM)

$$\mathrm{DOM} = \mathbf{C}_{\upsilon_k} - \hat{\mathbf{C}}_{\upsilon_k} \tag{31}$$

Kalman filtering with motion detection is important in target tracking applications. The innovation information at the present epoch can be employed for timely reflect the change in vehicle dynamic. Selecting the degree of divergence (DOD) as the trace of innovation covariance matrix at present epoch (i.e., the window size is one), we have:

$$\xi = \upsilon_k^{\mathrm{T}}\upsilon_k = tr(\upsilon_k\upsilon_k^{\mathrm{T}}) \tag{32}$$

This parameter can be utilized for detection of divergence/outliers or adaptation for adaptive filtering. If the discrepancy for the trace of innovation covariance matrix between the present (actual) and theoretical value is used, the DOD parameter can be of the form:

$$\eta = \mathbf{v}_k^{\mathrm{T}} \mathbf{v}_k - tr(\mathbf{C}_{v_k}) \tag{33}$$

The other DOD parameter commonly use as a simple test statistic for an occurrence of failure detection is based on the normalized innovation squared, defined as the ratio given by:

$$\mu = \frac{\mathbf{v}_k^{\mathrm{T}} \mathbf{v}_k}{tr(\mathbf{C}_{v_k})} = \mathbf{v}_k^{\mathrm{T}} \mathbf{C}_{v_k}^{-1} \mathbf{v}_k \tag{34}$$

For each of the approaches, only one scalar value needs to be determined, and therefore the fuzzy rules can be simplified resulting in the decrease of computational efficiency.

The logic of adaptation algorithm using covariance-matching technique is described as follows. When the actual covariance value $\hat{\mathbf{C}}_{v_k}$ is observed, if its value is within the range predicted by theory $\mathbf{C}_{v_k}$ and the difference is very near to zero, this indicates that both covariances match almost perfectly. If the actual covariance is greater than its theoretical value, the value of the process noise should be decreased; if the actual covariance is less than its theoretical value, the value of the process noise should be increased. The fuzzy logic (Abdelnour,et al , 1993; Jwo & Chang, 2007; Loebis, et al, 2007; Mostov & Soloviev, 1996; Sasiadek, et al, 2000) is popular mainly due to its simplicity even though some other approaches such as neural network and genetic algorithm may also be applicable. When the fuzzy logic approach based on rules of the kind:

IF〈antecedent〉THEN〈consequent〉

the following rules can be utilized to implement the idea of covariance matching:

A. $\hat{\mathbf{C}}_{v_k}$ is employed

(1) IF 〈 $\hat{\mathbf{C}}_{v_k} \approx 0$ 〉 THEN 〈 $\mathbf{Q}_k$ is unchanged〉 (This indicates that $\hat{\mathbf{C}}_{v_k}$ is near to zero, the process noise statistic should be remained.)

(2) IF 〈 $\hat{\mathbf{C}}_{v_k} > 0$ 〉 THEN 〈 $\mathbf{Q}_k$ is increased〉 (This indicates that $\hat{\mathbf{C}}_{v_k}$ is larger than zero, the process noise statistic is too small and should be increased.)

(3) IF 〈 $\hat{\mathbf{C}}_{v_k} < 0$ 〉 THEN 〈 $\mathbf{Q}_k$ is decreased〉 (This indicates that $\hat{\mathbf{C}}_{v_k}$ is less than zero, the process noise statistic is too large and should be decreased.)

B. DOM is employed

(1) IF 〈 DOM ≈ 0 〉 THEN 〈 $\mathbf{Q}_k$ is unchanged〉 (This indicates that $\hat{\mathbf{C}}_{v_k}$ is about the same as $\mathbf{C}_{v_k}$, the process noise statistic should be remained.)

(2) IF 〈 DOM > 0 〉 THEN 〈 $\mathbf{Q}_k$ is decreased〉 (This indicates that $\hat{\mathbf{C}}_{v_k}$ is less than $\mathbf{C}_{v_k}$, the process noise statistic should be decreased.)

(3) IF 〈 DOM < 0 〉 THEN 〈 $\mathbf{Q}_k$ is increased〉 (This indicates that $\hat{\mathbf{C}}_{v_k}$ is larger than $\mathbf{C}_{v_k}$, the process noise statistic should be increased.)

C. DOD (μ) is employed

Suppose that μ is employed as the test statistic, and μ_T represents the chosen threshold. The following fuzzy rules can be utilized:
(1) IF 〈 $\mu \geq \mu_T$ 〉 THEN 〈 $\mathbf{Q}_k$ is increased〉 (There is a failure or maneuvering reported; the process noise statistic is too small and needs to be increased)
(2) IF 〈 $\mu < \mu_T$ 〉 THEN 〈 $\mathbf{Q}_k$ is decreased〉 (There is no failure or non maneuvering; the process noise statistic is too large and needs to be decreased)

3. An IAE/AFKF Hybrid Approach

In this section, a hybrid approach (Jwo & Weng, 2008) involving the concept of the two methods is presented. The proposed method is a hybrid version of the IAE and AFKF approaches. The ratio of the actual innovation covariance based on the sampled sequence to the theoretical innovation covariance will be employed for dynamically tuning two filter parameters - fading factors and measurement noise scaling factors. The method has the merits of good computational efficiency and numerical stability. The matrices in the KF loop are able to remain positive definitive.
The conventional KF approach is coupled with the adaptive tuning system (ATS) for providing two system parameters: fading factor and noise covariance scaling factor. In the ATS mechanism, both adaptations on process noise covariance (also referred to P-adaptation herein) and on measurement noise covariance (also referred to R-adaptation herein) are involved. The idea is based on the concept that when the filter achieves estimation optimality, the actual innovation covariance based on the sampled sequence and the theoretical innovation covariance should be equal. In other words, the ratio between the two should equal one.
(1) Adaptation on process noise covariance.

To account for the uncertainty, the covariance matrix needs to be updated, through the following way. The new $\overline{\mathbf{P}}_k^-$ can be obtained by multiplying $\mathbf{P}_k^-$ by the factor $\boldsymbol{\lambda}_P$:

$$\overline{\mathbf{P}}_k^- = \boldsymbol{\lambda}_P \mathbf{P}_k^- \tag{35}$$

and the corresponding Kalman gain is given by

$$\overline{\mathbf{K}}_k = \overline{\mathbf{P}}_k^- \mathbf{H}_k^{\mathrm{T}} [\mathbf{H}_k \overline{\mathbf{P}}_k^- \mathbf{H}_k^{\mathrm{T}} + \overline{\mathbf{R}}_k]^{-1} \tag{36a}$$

If representing the new variable $\overline{\mathbf{R}}_k = \boldsymbol{\lambda}_R \mathbf{R}_k$, we have

$$\overline{\mathbf{K}}_k = \overline{\mathbf{P}}_k^- \mathbf{H}_k^{\mathrm{T}} [\mathbf{H}_k \overline{\mathbf{P}}_k^- \mathbf{H}_k^{\mathrm{T}} + \boldsymbol{\lambda}_R \mathbf{R}_k]^{-1} \tag{36b}$$

From Equation (36b), it can be seen that the change of covariance is essentially governed by two of the parameters: $\overline{\mathbf{P}}_k^-$ and $\mathbf{R}_k$. In addition, the covariance matrix at the measurement update stage, from Equation (7), can be written as

$$\overline{\mathbf{P}}_k = [\mathbf{I} - \overline{\mathbf{K}}_k \mathbf{H}_k] \overline{\mathbf{P}}_k^- \tag{37a}$$

and

$$\overline{\mathbf{P}}_k = \boldsymbol{\lambda}_P [\mathbf{I} - \overline{\mathbf{K}}_k \mathbf{H}_k] \mathbf{P}_k^- \tag{37b}$$

Furthermore, based on the relationship given by Equation (35), the covariance matrix at the prediction stage (i.e., Equation (4)) is given by

$$\overline{\mathbf{P}}_{k+1}^- = \boldsymbol{\Phi}_k \overline{\mathbf{P}}_k \boldsymbol{\Phi}_k^{\mathrm{T}} + \mathbf{Q}_k \tag{38}$$

or, alternatively

$$\overline{\mathbf{P}}_{k+1}^{-} = \boldsymbol{\lambda}_P \boldsymbol{\Phi}_k \mathbf{P}_k \boldsymbol{\Phi}_k^{\mathrm{T}} + \mathbf{Q}_k \tag{39a}$$

On the other hand, the covariance matrix can also be approximated by

$$\overline{\mathbf{P}}_{k+1}^{-} = \boldsymbol{\lambda}_P \mathbf{P}_{k+1}^{-} = \boldsymbol{\lambda}_P (\boldsymbol{\Phi}_k \mathbf{P}_k \boldsymbol{\Phi}_k^{T} + \mathbf{Q}_k) \tag{39b}$$

where $\boldsymbol{\lambda}_P = diag(\lambda_1, \lambda_2 \ldots, \lambda_m)$. The main difference between different adaptive fading algorithms is on the calculation of scale factor $\boldsymbol{\lambda}_P$. One approach is to assign the scale factors as constants. When $\lambda_i \le 1$ ($i = 1,2,\ldots,m$), the filtering is in a steady state processing while $\lambda_i > 1$, the filtering may tend to be unstable. For the case $\lambda_i = 1$, it deteriorates to the standard Kalman filter. There are some drawbacks with constant factors, e.g., as the filtering proceeds, the precision of the filtering will decrease because the effects of old data tend to become less and less. The ideal way is to use time varying factors that are determined according to the dynamic and observation model accuracy.

When there is deviation due to the changes of covariance and measurement noise, the corresponding innovation covariance matrix can be rewritten as:

$$\overline{\mathbf{C}}_{\upsilon_k} = \mathbf{H}_k \overline{\mathbf{P}}_k^{-} \mathbf{H}_k^{\mathrm{T}} + \overline{\mathbf{R}}_k$$

and

$$\overline{\mathbf{C}}_{\upsilon_k} = \boldsymbol{\lambda}_P \mathbf{H}_k \mathbf{P}_k^{-} \mathbf{H}_k^{\mathrm{T}} + \boldsymbol{\lambda}_R \mathbf{R}_k \tag{40}$$

To enhance the tracking capability, the time-varying suboptimal scaling factor is incorporated, for on-line tuning the covariance of the predicted state, which adjusts the filter gain, and accordingly the improved version of AFKF is obtained. The optimum fading factors can be calculated through the single factor:

$$\lambda_i = (\boldsymbol{\lambda}_P)_{ii} = \max\left\{1, \frac{tr(\hat{\mathbf{C}}_{\upsilon_k})}{tr(\mathbf{C}_{\upsilon_k})}\right\},\ i = 1,2\ldots,m \tag{41}$$

where $tr[\cdot]$ is the trace of matrix; $\lambda_i \ge 1$, is a scaling factor. Increasing λ_i will improve tracking performance.

(2) Adaptation on measurement noise covariance. As the strength of measurement noise changes with the environment, incorporation of the fading factor only is not able to restrain the expected estimation accuracy. For resolving these problems, the ATS needs a mechanism for R-adaptation in addition to P-adaptation, to adjust the noise strengths and improve the filter estimation performance.

A parameter which represents the ratio of the actual innovation covariance based on the sampled sequence to the theoretical innovation covariance matrices can be defined as one of the following methods:

(a) Single factor

$$\lambda_j = (\boldsymbol{\lambda}_R)_{jj} = \frac{tr(\hat{\mathbf{C}}_{\upsilon_k})}{tr(\mathbf{C}_{\upsilon_k})},\ j = 1,2\ldots,n \tag{42a}$$

(b) Multiple factors

$$\lambda_j = \frac{(\hat{\mathbf{C}}_{\upsilon_k})_{jj}}{(\mathbf{C}_{\upsilon_k})_{jj}},\ j = 1,2\ldots,n \tag{42b}$$

It should be noted that from Equation (40) that increasing $\mathbf{R}_k$ will lead to increasing $\mathbf{C}_{\upsilon_k}$, and vice versa. This means that time-varying $\mathbf{R}_k$ leads to time-varying $\mathbf{C}_{\upsilon_k}$. The value of $\boldsymbol{\lambda}_R$ is introduced in order to reduce the discrepancies between $\mathbf{C}_{\upsilon_k}$ and $\mathbf{R}_k$. The adaptation can be implemented through the simple relation:

$$\overline{\mathbf{R}}_k = \boldsymbol{\lambda}_R \mathbf{R}_k \tag{43}$$

Further detail regarding the adaptive tuning loop is illustrated by the flow charts shown in Figs. 1 and 2, where two architectures are presented. Fig. 1 shows the system architecture #1 and Fig. 2 shows the system architecture #2, respectively. In Fig. 1, the flow chart contains two portions, for which the block indicated by the dot lines is the adaptive tuning system (ATS) for tuning the values of both P and R parameters; in Fig. 2, the flow chart contains three portions, for which the two blocks indicated by the dot lines represent the R-adaptation loop and P-adaptation loop, respectively.

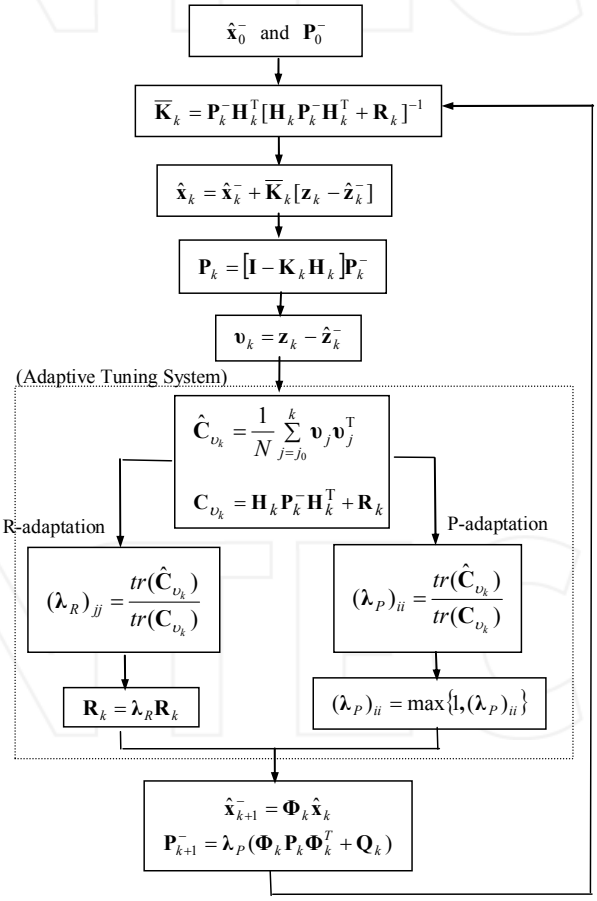

Fig. 1. Flow chart of the IAE/AFKF hybrid AKF method - system architecture #1

An important remark needs to be pointed out. When the system architecture #1 is employed, only one window size is needed. It can be seen that the measurement noise covariance of the innovation covariance matrix hasn't been updated when performing the fading factor calculation. In the system architecture #2, the latest information of the measurement noise strength has already been available when performing the fading factor calculation. However, one should notice that utilization of the 'old' (i.e., before R-adaptation) information is required. Otherwise, unreliable result may occur since the deviation of the innovation covariance matrix due to the measurement noise cannot be correctly detected. One strategy for avoiding this problem can be done by using two different window sizes, one for R-adaptation loop and the other for P-adaptation loop.

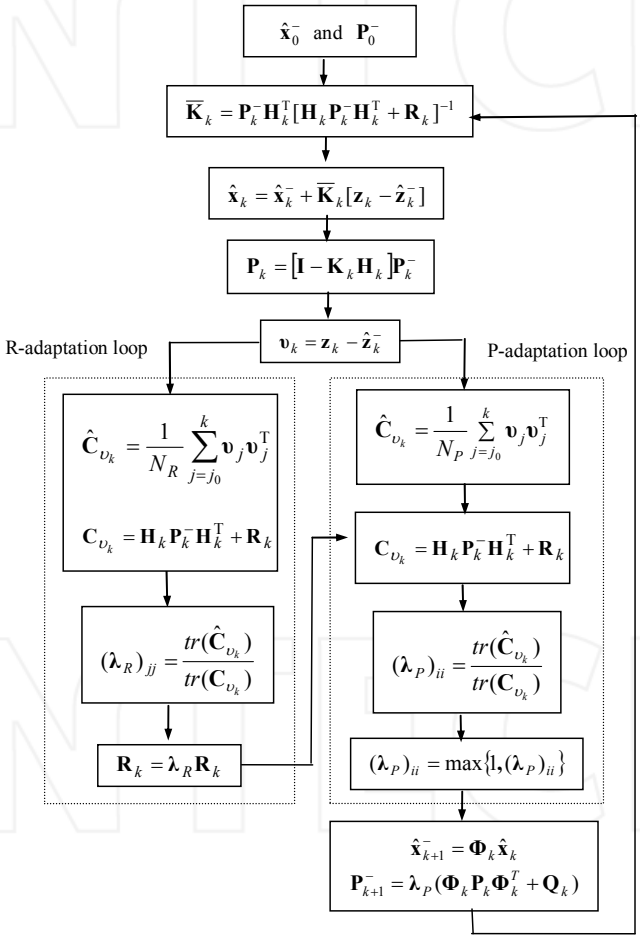

Fig. 2. Flow chart of the IAE/AFKF hybrid AKF method - system architecture #2

4. Navigation Sensor Fusion Example

In this section, two illustrative examples for GPS/INS navigation sensor fusion are provided. The loosely-coupled GPS/INS architecture is employed for demonstration. Simulation experiments were conducted using a personal computer. The computer codes were constructed using the Matlab® software. The commercial software Satellite Navigation (SATNAV) Toolbox by GPSoft LLC was used for generating the satellite positions and pseudoranges. The satellite constellation was simulated and the error sources corrupting GPS measurements include ionospheric delay, tropospheric delay, receiver noise and multipath. Assume that the differential GPS mode is used and most of the errors can be corrected, but the multipath and receiver thermal noise cannot be eliminated.

The differential equations describing the two-dimensional inertial navigation state are (Farrell, 1998):

$$\begin{bmatrix} \dot{n} \\ \dot{e} \\ \dot{v}_n \\ \dot{v}_e \\ \dot{\psi} \end{bmatrix} = \begin{bmatrix} v_n \\ v_e \\ a_n \\ a_e \\ \omega_r \end{bmatrix} = \begin{bmatrix} v_n \\ v_e \\ \cos(\psi)a_u - \sin(\psi)a_v \\ \sin(\psi)a_u + \cos(\psi)a_v \\ \omega_r \end{bmatrix} \tag{44}$$

where [a_u , a_v] are the measured accelerations in the body frame, ω_r is the measured yaw rate in the body frame, as shown in Fig. 3. The error model for INS is augmented by some sensor error states such as accelerometer biases and gyroscope drifts. Actually, there are several random errors associated with each inertial sensor. It is usually difficult to set a certain stochastic model for each inertial sensor that works efficiently at all environments and reflects the long-term behavior of sensor errors. The difficulty of modeling the errors of INS raised the need for a model-less GPS/INS integration technique. The linearized equations for the process model can be selected as

$$\frac{d}{dt}\begin{bmatrix} \delta n \\ \delta e \\ \delta v_n \\ \delta v_e \\ \delta\psi \\ \delta a_u \\ \delta a_v \\ \delta\omega_r \end{bmatrix} = \begin{bmatrix} 0 & 0 & 1 & 0 & 0 & 0 & 0 & 0 \\ 0 & 0 & 0 & 1 & 0 & 0 & 0 & 0 \\ 0 & 0 & 0 & 0 & -a_e & \cos(\psi) & -\sin(\psi) & 0 \\ 0 & 0 & 0 & 0 & -a_n & \sin(\psi) & \cos(\psi) & 0 \\ 0 & 0 & 0 & 0 & 0 & 0 & 0 & 1 \\ 0 & 0 & 0 & 0 & 0 & 0 & 0 & 0 \\ 0 & 0 & 0 & 0 & 0 & 0 & 0 & 0 \\ 0 & 0 & 0 & 0 & 0 & 0 & 0 & 0 \end{bmatrix} \begin{bmatrix} \delta n \\ \delta e \\ \delta v_n \\ \delta v_e \\ \delta\psi \\ \delta a_u \\ \delta a_v \\ \delta\omega_r \end{bmatrix} + \begin{bmatrix} 0 \\ 0 \\ u_{acc} \\ u_{acc} \\ u_{gyro} \\ u^b_{acc} \\ u^b_{acc} \\ u^b_{gyro} \end{bmatrix} \tag{45}$$

which can be utilized in the integration Kalman filter as the inertial error model. In Equation (45), δn and δe represent the east, and north position errors; δv_n and δv_e represent the east, and north velocity errors; $\delta\psi$ represents yaw angle; δa_u , δa_v , and $\delta\omega_r$ represent the accelerometer biases and gyroscope drift, respectively. The measurement model can be written as

$$\mathbf{z}_k = \begin{bmatrix} n_{INS} \\ e_{INS} \end{bmatrix} - \begin{bmatrix} n_{GPS} \\ e_{GPS} \end{bmatrix} = \begin{bmatrix} 1 & 0 & 0 & 0 & 0 & 0 & 0 & 0 \\ 0 & 1 & 0 & 0 & 0 & 0 & 0 & 0 \end{bmatrix} \begin{bmatrix} \delta n \\ \delta e \\ \delta v_n \\ \delta v_e \\ \delta \psi \\ \delta a_u \\ \delta a_v \\ \delta \omega_r \end{bmatrix} + \begin{bmatrix} v_n \\ v_e \end{bmatrix} \tag{46}$$

Further simplification of the above two models leads to

$$\frac{d}{dt} \begin{bmatrix} \delta n \\ \delta e \\ \delta v_n \\ \delta v_e \\ \delta \psi \end{bmatrix} = \begin{bmatrix} 0 & 0 & 1 & 0 & 0 \\ 0 & 0 & 0 & 1 & 0 \\ 0 & 0 & 0 & 0 & 0 \\ 0 & 0 & 0 & 0 & 0 \\ 0 & 0 & 0 & 0 & 0 \end{bmatrix} \begin{bmatrix} \delta n \\ \delta e \\ \delta v_n \\ \delta v_e \\ \delta \psi \end{bmatrix} + \begin{bmatrix} 0 \\ 0 \\ w_n \\ w_e \\ w_\psi \end{bmatrix} \tag{47}$$

and

$$\mathbf{z}_k = \begin{bmatrix} n_{INS} \\ e_{INS} \end{bmatrix} - \begin{bmatrix} n_{GPS} \\ e_{GPS} \end{bmatrix} = \begin{bmatrix} 1 & 0 & 0 & 0 & 0 \\ 0 & 1 & 0 & 0 & 0 \end{bmatrix} \begin{bmatrix} \delta n \\ \delta e \\ \delta v_n \\ \delta v_e \\ \delta \psi \end{bmatrix} + \begin{bmatrix} v_n \\ v_e \end{bmatrix} \tag{48}$$

respectively.

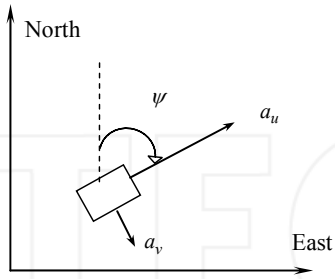

Fig. 3. Two-dimensional inertial navigation, Farrell & Barth (1999)

(A) Example 1: utilization of the fuzzy adaptive fading Kalman filter (FAFKF) approach
The first illustrative example is taken from Jwo & Huang (2009). Fig. 4 provides the strategy for the GPS/INS navigation processing based on the FAFKF mechanism. The GPS navigation solution based on the least-squares (LS) is solved at the first stage. The measurement is the residual between GPS LS and INS derived data, which is used as the measurement of the KF.

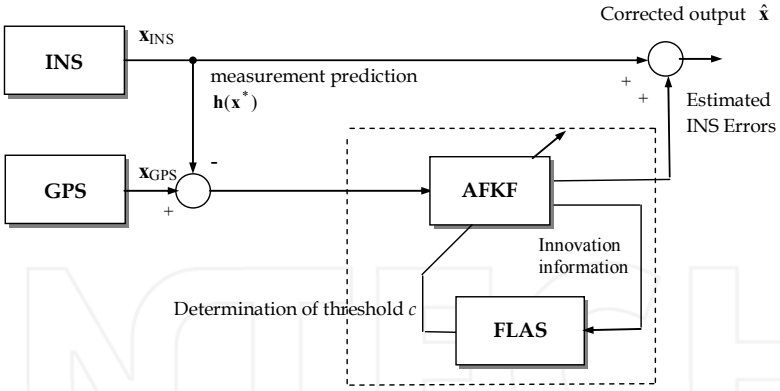

Fig. 4. GPS/INS navigation processing using the FAFKF for the illustrative example 1.

The experiment was conducted on a simulated vehicle trajectory originating from the (0, 0) m location. The simulated trajectory of the vehicle and the INS derived position are shown as in Fig. 5. The trajectory of the vehicle can be approximately divided into two categories according to the dynamic characteristics. The vehicle was simulated to conduct constant-velocity straight-line during the three time intervals, 0-200, 601-1000 and 1401-1600s, all at a speed of 10π m/s. Furthermore, it conducted counterclockwise circular motion with radius 2000 meters during 201-600 and 1001-1400s where high dynamic maneuvering is involved. The following parameters were used: window size N =10; the values of noise standard deviation are 2e-3 m/s^2 for accelerometers and 5e-4 m/s^2 for gyroscopes.
The presented FLAS is the *If-Then* form and consists of 3 rules. The $\bar{\boldsymbol{\upsilon}}$ and innovation covariance $\hat{\mathbf{C}}_{\upsilon_k}$ as the inputs. The fuzzy rules are designed as follows:

1. If $\bar{\boldsymbol{\upsilon}}$ is zero and $\hat{\mathbf{C}}_{\upsilon_k}$ is zero then c is large
2. If $\bar{\boldsymbol{\upsilon}}$ is zero and $\hat{\mathbf{C}}_{\upsilon_k}$ is small then c is large
3. If $\bar{\boldsymbol{\upsilon}}$ is zero and $\hat{\mathbf{C}}_{\upsilon_k}$ is large then c is small
4. If $\bar{\boldsymbol{\upsilon}}$ is small and $\hat{\mathbf{C}}_{\upsilon_k}$ is zero then c is small
5. If $\bar{\boldsymbol{\upsilon}}$ is small and $\hat{\mathbf{C}}_{\upsilon_k}$ is small then c is small
6. If $\bar{\boldsymbol{\upsilon}}$ is small and $\hat{\mathbf{C}}_{\upsilon_k}$ is large then c is zero
7. If $\bar{\boldsymbol{\upsilon}}$ is large and $\hat{\mathbf{C}}_{\upsilon_k}$ is zero then c is zero
8. If $\bar{\boldsymbol{\upsilon}}$ is large and $\hat{\mathbf{C}}_{\upsilon_k}$ is small then c is zero
9. If $\bar{\boldsymbol{\upsilon}}$ is large and $\hat{\mathbf{C}}_{\upsilon_k}$ is large then c is zero

The triangle membership functions for innovation mean value ($\bar{\boldsymbol{\upsilon}}$), innovation covariance ($\hat{\mathbf{C}}_{\upsilon_k}$) and threshold ($c$) are shown in Fig. 6. The center of area approach was used for the defuzzification. Fig. 7 shows the East and North components of navigation errors and the corresponding 1-σ bounds based on the AFKF method and FAFKF method, respectively. Fig. 8 provides the navigation accuracy comparison for AFKF and FAFKF. Fig. 9 gives the trajectories of the threshold c (the fuzzy logic output), and the corresponding fading factor λ_k, respectively.

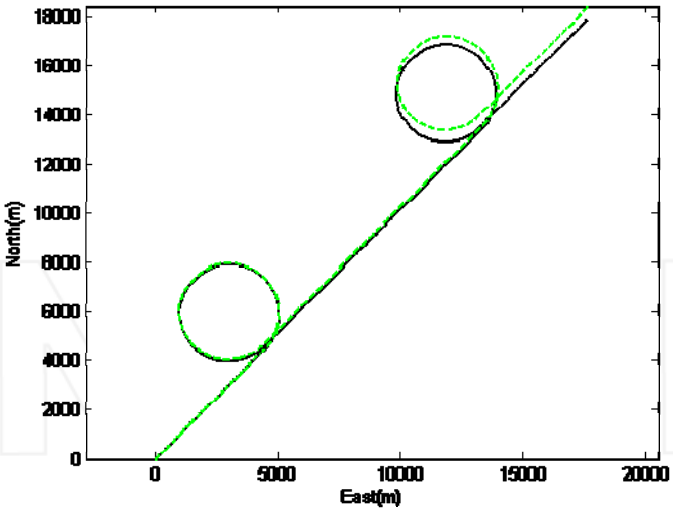

Fig. 5. Trajectory for the simulated vehicle (solid) and the INS derived position (dashed)

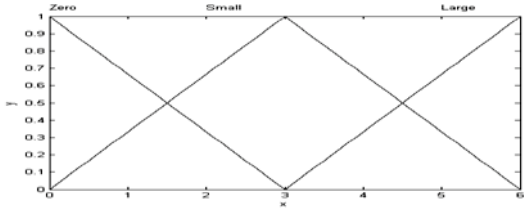

(a) Innovation mean value ($\bar{\upsilon}$)

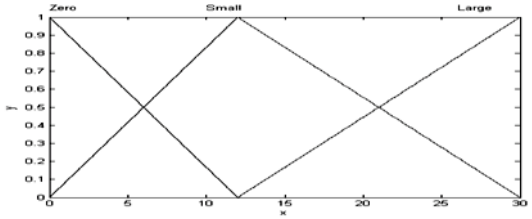

(b) Innovation covariance ($\hat{\mathbf{C}}_{\upsilon_k}$)

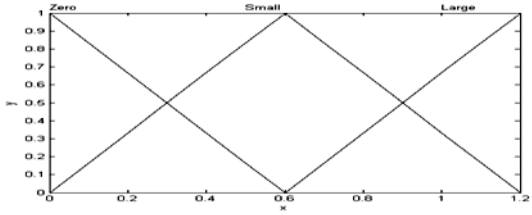

(c) Threshold c

Fig. 6. Membership functions for the inputs and output

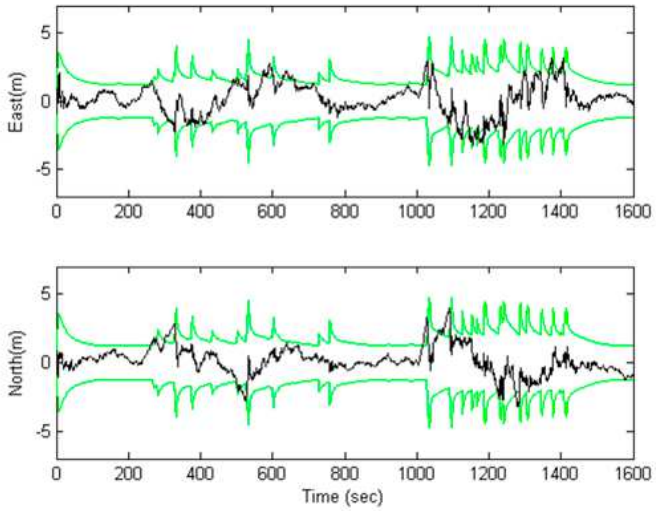

Fig. 7. East and north components of navigation errors and the 1-σ bound based on the FAFKF method

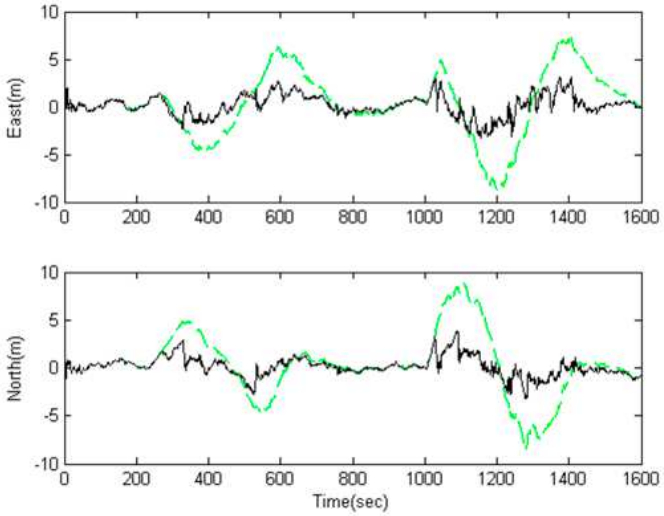

Fig. 8. Navigation accuracy comparison for AFKF and FAFKF

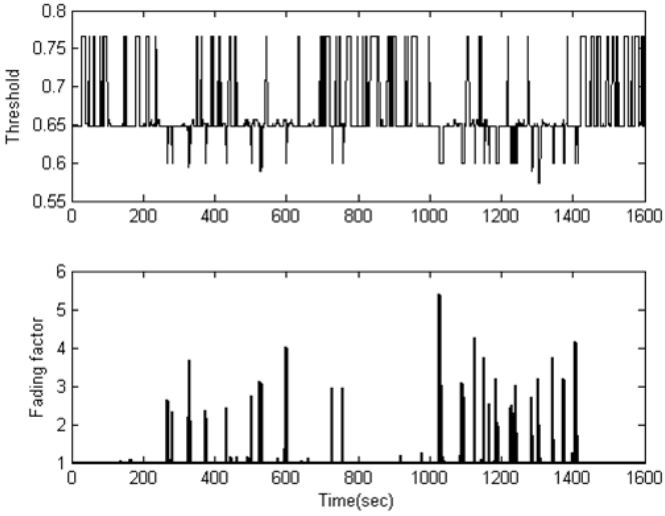

Fig. 9. Trajectories of the threshold c (top) from the fuzzy logic output, and the corresponding fading factor λ_k (bottom)

(B) Example 2: utilization of the IAE/AFKF Hybrid approach

The second example is taken from Jwo & Weng (2008). Fig. 10 shows the GPS/INS navigation processing using the IAE/AFKF Hybrid AKF. Trajectory for the simulated vehicle (solid) and the unaided INS derived position (dashed) is shown in Fig. 11. The trajectory of the vehicle can be approximately divided into two categories according to the dynamic characteristics. The vehicle was simulated to conduct constant-velocity straight-line during the three time intervals, 0-300, 901-1200 and 1501-1800s, all at a speed of 10π m/s. Furthermore, it conducted counterclockwise circular motion with radius 3000 meters during 301-900, and 1201-1500s where high dynamic maneuvering is involved. The following parameters were used: window size $N_p = 15$ $N_R = 20$; the values of noise standard deviation are 1e-3 m/s^2 for accelerometers and gyroscopes.

Fig. 12 provides the positioning solution from the integrated navigation system (without adaptation) as compared to the GPS navigation solutions by the LS approach, while Fig. 13 gives the positioning results for the integrated navigation system with and without adaptation. Substantial improvement in navigation accuracy can be obtained.

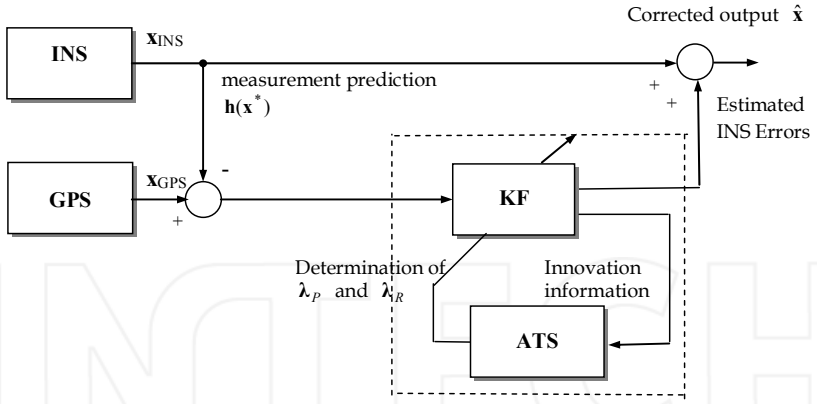

Fig. 10. GPS/INS navigation processing using the IAE/AFKF Hybrid AKF for the illustrative example 2

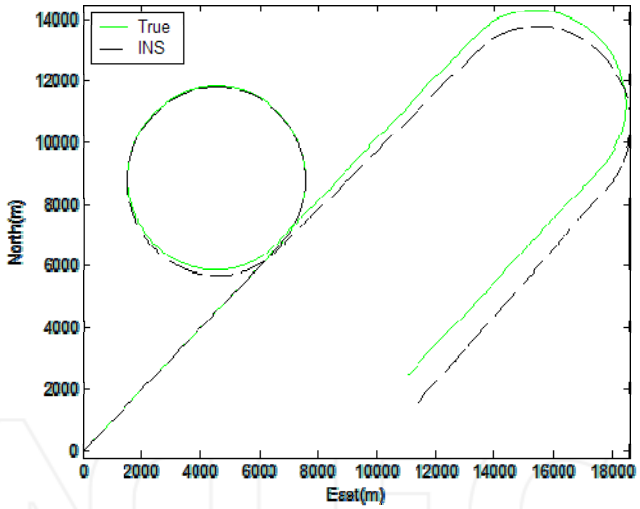

Fig. 11. Trajectory for the simulated vehicle (solid) and the INS derived position (dashed)

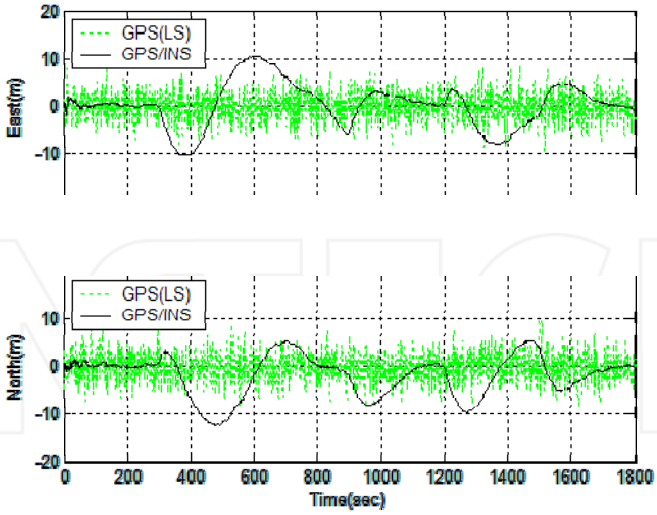

Fig. 12. The solution from the integrated navigation system without adaptation as compared to the GPS navigation solutions by the LS approach

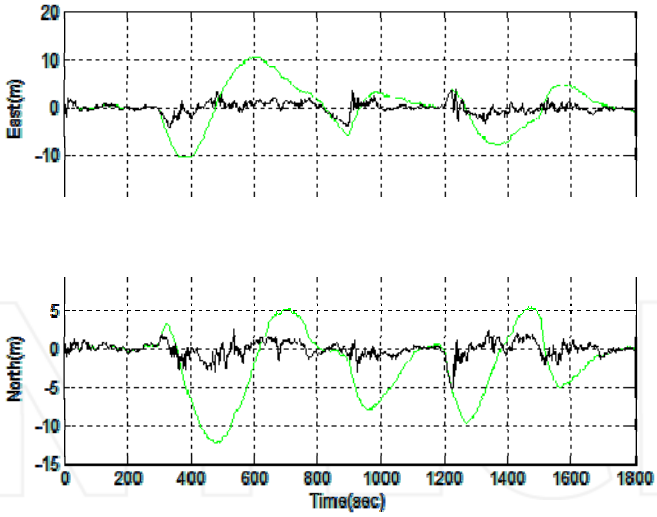

Fig. 13. The solutions for the integrated navigation system with and without adaptation

In the real world, the measurement will normally be changing in addition to the change of process noise or dynamic such as maneuvering. In such case, both P-adaptation and R-adaptation tasks need to be implemented. In the following discussion, results will be provided for the case when measurement noise strength is changing in addition to the

change of process noise strength. The measurement noise strength is assumed to be changing with variances of the values $r = 4^2 \rightarrow 16^2 \rightarrow 8^2 \rightarrow 3^2$, where the 'arrows (→)' is employed for indicating the time-varying trajectory of measurement noise statistics. That is, it is assumed that the measure noise strength is changing during the four time intervals: 0-450s ($N(0,4^2)$), 451-900s ($N(0,16^2)$), 901-1350s ($N(0,8^2)$), and 1351-1800s ($N(0,3^2)$). However, the internal measurement noise covariance matrix $\mathbf{R}_k$ is set unchanged all the time in simulation, which uses $r_j \sim N(0,3^2)$, $j = 1,2\ldots,n$, at all the time intervals.

Fig. 14 shows the east and north components of navigation errors and the 1-σ bound based on the method without adaptation on measurement noise covariance matrix. It can be seen that the adaptation of P information without correct R information (referred to partial adaptation herein) seriously deteriorates the estimation result. Fig. 15 provides the east and north components of navigation errors and the 1-σ bound based on the proposed method (referred to full adaptation herein, i.e., adaptation on both estimation covariance and measurement noise covariance matrices are applied). It can be seen that the estimation accuracy has been substantially improved. The measurement noise strength has been accurately estimated, as shown in Fig. 16.

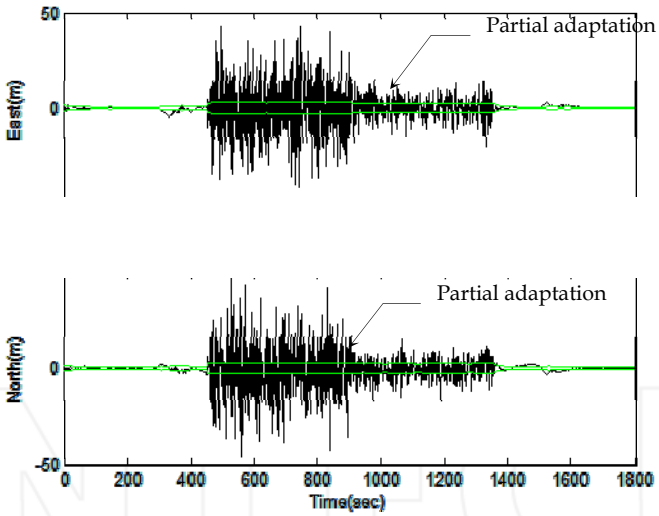

Fig. 14. East and north components of navigation errors and the 1-σ bound based on the method without measurement noise adaptation

It should also be mentioned that the requirement $(\boldsymbol{\lambda}_P)_{ii} \geq 1$ is critical. An illustrative example is given in Figs. 17 and 18. Fig. 17 gives the navigation errors and the 1-σ bound when the threshold setting is not incorporated. The corresponding reference (true) and calculated standard deviations when the threshold setting is not incorporated is provided in Fig. 18. It is not surprising that the navigation accuracy has been seriously degraded due to the inaccurate estimation of measurement noise statistics.

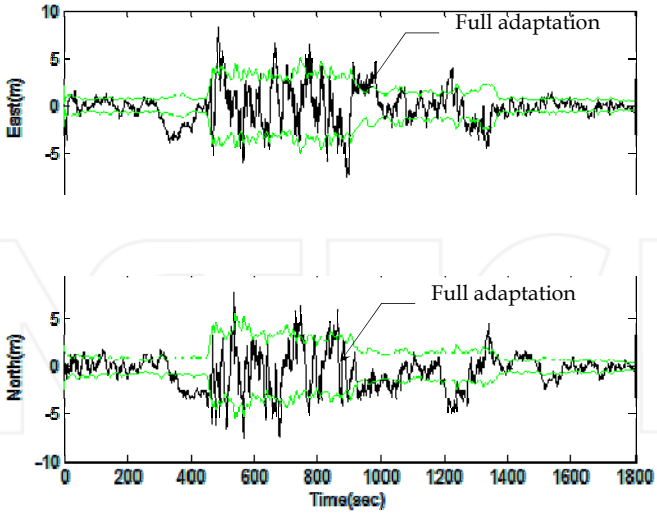

Fig. 15. East and north components of navigation errors and the 1-σ bound based on the proposed method (with adaptation on both estimation covariance and measurement noise covariance matrices)

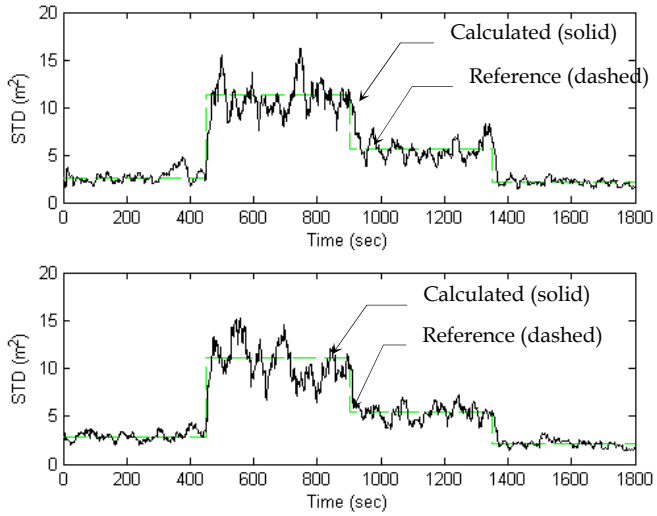

Fig. 16. Reference (true) and calculated standard deviations for the east (top) and north (bottom) components of the measurement noise variance values

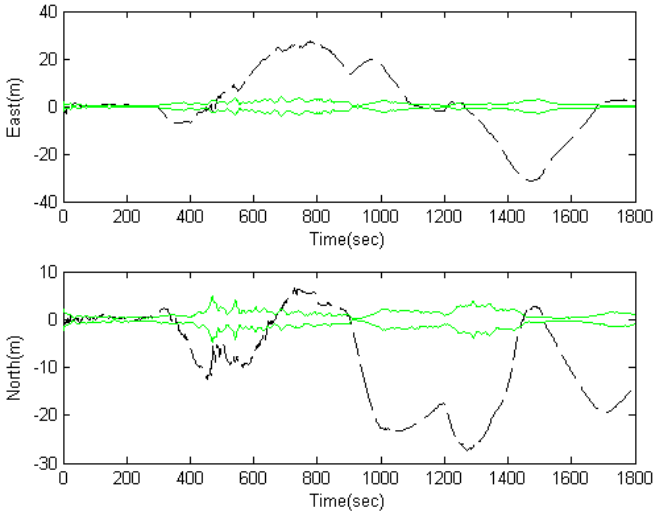

Fig. 17. East and north components of navigation errors and the 1-σ bound based on the proposed method when the threshold setting is not incorporated

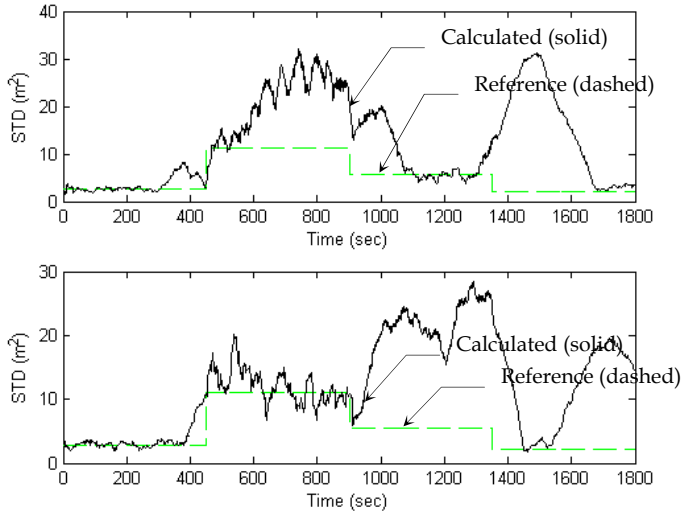

Fig. 18. Reference (true) and calculated standard deviations for the east and north components of the measurement noise variance values when the threshold setting is not incorporated

5. Conclusion

This chapter presents the adaptive Kalman filter for navigation sensor fusion. Several types of adaptive Kalman filters has been reviewed, including the innovation-based adaptive estimation (IAE) approach and the adaptive fading Kalman filter (AFKF) approach. Various types of designs for the fading factors are discussed. A new strategy through the hybridization of IAE and AFKF is presented with an illustrative example for integrated navigation application. In the first example, the fuzzy logic is employed for assisting the AFKF. Through the use of fuzzy logic, the designed fuzzy logic adaptive system (FLAS) has been employed as a mechanism for timely detecting the dynamical changes and implementing the on-line tuning of threshold c , and accordingly the fading factor, by monitoring the innovation information so as to maintain good tracking capability.

In the second example, the conventional KF approach is coupled by the adaptive tuning system (ATS), which gives two system parameters: the fading factor and measurement noise covariance scaling factor. The ATS has been employed as a mechanism for timely detecting the dynamical and environmental changes and implementing the on-line parameter tuning by monitoring the innovation information so as to maintain good tracking capability and estimation accuracy. Unlike some of the AKF methods, the proposed method has the merits of good computational efficiency and numerical stability. The matrices in the KF loop are able to remain positive definitive. Remarks to be noted for using the method is made, such as: (1) The window sizes can be set different, to avoid the filter degradation/divergence; (2) The fading factors $(\boldsymbol{\lambda}_P)_{ii}$ should be always larger than one while $(\boldsymbol{\lambda}_R)_{jj}$ does not have such limitation.

Simulation experiments for navigation sensor fusion have been provided to illustrate the accessibility. The accuracy improvement based on the AKF method has demonstrated remarkable improvement in both navigational accuracy and tracking capability.

6. References

Abdelnour, G.; Chand, S. & Chiu, S. (1993). Applying fuzzy logic to the Kalman filter divergence problem. *IEEE Int. Conf. On Syst., Man and Cybernetics, Le Touquet, France,* pp. 630-634

Brown, R. G. & Hwang, P. Y. C. (1997). *Introduction to Random Signals and Applied Kalman Filtering,* John Wiley & Sons, New York, 3rd edn

Bar-Shalom, Y.; Li, X. R. & Kirubarajan, T. (2001). *Estimation with Applications to Tracking and Navigation,* John Wiley & Sons, Inc

Bakhache, B. & Nikiforov, I. (2000). Reliable detection of faults in measurement systems, *International Journal of adaptive control and signal processing*, 14, pp. 683-700

Caliskan, F. & Hajiyev, C. M. (2000). Innovation sequence application to aircraft sensor fault detection: comparison of checking covariance matrix algorithms, *ISA Transactions,* 39, pp. 47-56

Ding, W.; Wang, J. & Rizos, C. (2007). Improving Adaptive Kalman Estimation in GPS/INS Integration, *The Journal of Navigation*, 60, 517-529.

Farrell, I. & Barth, M. (1999) *The Global Positioning System and Inertial Navigation*, McCraw-Hill professional, New York

Gelb, A. (1974). *Applied Optimal Estimation*. M. I. T. Press, MA.

Grewal, M. S. & Andrews, A. P. (2001). *Kalman Filtering, Theory and Practice Using MATLAB*, 2nd Ed., John Wiley & Sons, Inc.

Hide, C, Moore, T., & Smith, M. (2003). Adaptive Kalman filtering for low cost INS/GPS, *The Journal of Navigation*, 56, 143-152

Jwo, D.-J. & Cho, T.-S. (2007). A practical note on evaluating Kalman filter performance Optimality and Degradation. *Applied Mathematics and Computation, 193,* pp. 482-505

Jwo, D.-J. & Wang, S.-H. (2007). Adaptive fuzzy strong tracking extended Kalman filtering for GPS navigation, *IEEE Sensors Journal*, 7(5), pp. 778-789

Jwo, D.-J. & Weng, T.-P. (2008). An adaptive sensor fusion method with applications in integrated navigation. *The Journal of Navigation*, 61, pp. 705-721

Jwo, D.-J. & Chang, F.-I., 2007, A Fuzzy Adaptive Fading Kalman Filter for GPS Navigation, *Lecture Notes in Computer Science*, LNCS 4681:820-831, Springer-Verlag Berlin Heidelberg.

Jwo, D.-J. & Huang, C. M. (2009). A Fuzzy Adaptive Sensor Fusion Method for Integrated Navigation Systems, *Advances in Systems Science and Applications*, 8(4), pp.590-604.

Loebis, D.; Naeem, W.; Sutton, R.; Chudley, J. & Tetlow S. (2007). Soft computing techniques in the design of a navigation, guidance and control system for an autonomous underwater vehicle, *International Journal of adaptive control and signal processing*, 21:205-236

Mehra, R. K. (1970). On the identification of variance and adaptive Kalman filtering. *IEEE Trans. Automat. Contr., AC-15,* pp. 175-184

Mehra, R. K. (1971). On-line identification of linear dynamic systems with applications to Kalman filtering. *IEEE Trans. Automat. Contr.,* AC-16, pp. 12-21

Mehra, R. K. (1972). Approaches to adaptive filtering. *IEEE Trans. Automat. Contr.*, Vol. AC-17, pp. 693-698

Mohamed, A. H. & Schwarz K. P. (1999). Adaptive Kalman filtering for INS/GPS. *Journal of Geodesy, 73 (4),* pp. 193-203

Mostov, K. & Soloviev, A. (1996). Fuzzy adaptive stabilization of higher order Kalman filters in application to precision kinematic GPS, *ION GPS-96,* Vol. 2, pp. 1451-1456, Kansas

Salychev, O. (1998). *Inertial Systems in Navigation and Geophysics*, Bauman MSTU Press, Moscow.

Sasiadek, J. Z.; Wang, Q. & Zeremba, M. B. (2000). Fuzzy adaptive Kalman filtering for INS/GPS data fusion. *15th IEEE int. Symp. on intelligent control, Rio Patras, Greece,* pp. 181-186

Xia, Q.; Rao, M.; Ying, Y. & Shen, X. (1994). Adaptive fading Kalman filter with an application, *Automatica*, 30, pp. 1333-1338

Yang, Y.; He H. & Xu, T. (1999). Adaptively robust filtering for kinematic geodetic positioning, *Journal of Geodesy*, 75, pp.109-116

Yang, Y. & Xu, T. (2003). An adaptive Kalman filter based on Sage windowing weights and variance components, *The Journal of Navigation*, 56(2), pp. 231-240

Yang, Y.; Cui, X., & Gao, W. (2004). Adaptive integrated navigation for multi-sensor adjustment outputs, *The Journal of Navigation*, 57(2), pp. 287-295

Zhou, D. H. & Frank, P. H. (1996). Strong tracking Kalman filtering of nonlinear time-varying stochastic systems with coloured noise: application to parameter estimation and empirical robustness analysis. *Int. J. control,* Vol. 65, No. 2, pp. 295-307

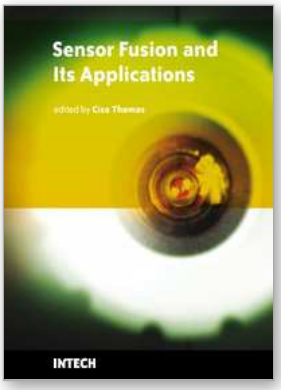

Sensor Fusion and its Applications

Edited by Ciza Thomas

ISBN 978-953-307-101-5
Hard cover, 488 pages
Publisher Sciyo
Published online 16, August, 2010
Published in print edition August, 2010

This book aims to explore the latest practices and research works in the area of sensor fusion. The book intends to provide a collection of novel ideas, theories, and solutions related to the research areas in the field of sensor fusion. This book is a unique, comprehensive, and up-to-date resource for sensor fusion systems designers. This book is appropriate for use as an upper division undergraduate or graduate level text book. It should also be of interest to researchers, who need to process and interpret the sensor data in most scientific and engineering fields. The initial chapters in this book provide a general overview of sensor fusion. The later chapters focus mostly on the applications of sensor fusion. Much of this work has been published in refereed journals and conference proceedings and these papers have been modified and edited for content and style. With contributions from the world's leading fusion researchers and academicians, this book has 22 chapters covering the fundamental theory and cutting-edge developments that are driving this field.

How to reference

In order to correctly reference this scholarly work, feel free to copy and paste the following:

Dah-Jing Jwo, Fong-Chi Chung and Tsu-Pin Weng (2010). Adaptive Kalman Filter for Navigation Sensor Fusion, Sensor Fusion and its Applications, Ciza Thomas (Ed.), ISBN: 978-953-307-101-5, InTech, Available from: http://www.intechopen.com/books/sensor-fusion-and-its-applications/adaptive-kalman-filter-for-navigation-sensor-fusion

INTECH
open science | open minds

InTech Europe
University Campus STeP Ri
Slavka Krautzeka 83/A
51000 Rijeka, Croatia
Phone: +385 (51) 770 447
Fax: +385 (51) 686 166
www.intechopen.com

InTech China
Unit 405, Office Block, Hotel Equatorial Shanghai
No.65, Yan An Road (West), Shanghai, 200040, China
中国上海市延安西路65号上海国际贵都大饭店办公楼405单元
Phone: +86-21-62489820
Fax: +86-21-62489821